Optics Letters

Femtosecond-written volume Bragg gratings in fluoride glasses

Lauris Talbot,[1,*] **Daniel Richter,**[2] **Maximilian Heck,**[2] **Stefan Nolte,**[2,3] ⬤ **and Martin Bernier**[1]

[1]*Centre d'Optique, Photonique et Laser (COPL), Université Laval, Québec City, Québec G1V 0A6, Canada*
[2]*Institute of Applied Physics, Abbe Center of Photonics, Friedrich-Schiller-Universität Jena, Albert-Einstein-Str. 15, 07745 Jena, Germany*
[3]*Fraunhofer Institute for Applied Optics and Precision Engineering, Albert-Einstein-Str. 7, 07745 Jena, Germany*
Corresponding author: lauris.talbot.1@ulaval.ca

We report on what we believe are the first volume Bragg gratings written inside bulk multicomponent fluoride glasses. The gratings inscribed with tightly focused infrared (IR)-femtosecond pulses in combination with the phase-mask technique exhibit refractive index modulations of up to 5×10^{-4} with reflectivities up to 90% at a wavelength near 2.8 μm. Such highly compact and narrowband filters could have a significant impact on numerous high-end applications from the UV to the mid-IR. © 2020 Optical Society of America

Volume Bragg gratings (VBGs) have gained growing interest over the last decades mainly as wavelength-stabilization elements for laser diodes as well as beam combiners for high-power lasers [1,2]. So far, VBGs have been realized based on the photo-inscription of either photo-thermo-refractive glasses with UV light [3] or also various other materials by using femtosecond (fs) laser pulses [4–7]. This last technique is especially interesting as it enables a confined and precise grating implementation into a broad range of non-photosensitive materials due to nonlinear absorption processes that are triggered in the focal volume [8]. To induce the required refractive index modulation, the simplest approach is by means of a microscope objective where an array of separated lines inscribed one after the other is implemented inside the bulk. With this technique, VBGs have been implemented into various materials such as fused silica [4], borosilicate [5], PMMA [6], and chalcogenide glasses [7] showing high diffraction efficiencies. However, the period of these gratings is usually in the range of a few microns, which is not desirable for VBGs that work in reflection in the range of the near-infrared and the short wavelength part of the mid-infrared (mid-IR). Above all, these gratings generally exhibit a poor period stability and have, therefore, so far, only been used as diffraction gratings [9]. These limitations can be overcome with another convenient and widespread method, which uses a two-beam interference pattern generated by a phase mask [10]. VBGs in fused silica with outstanding diffraction and reflection efficiencies were fabricated using this technique [2,9].

In recent years and in addition to the materials mentioned above, multicomponent fluoride glasses have been attracting more and more attention due to their large transparency window spanning from the UV to the mid-IR wavelength region [11]. The latter portion of the spectrum is of high interest for a wide range of applications in medicine, spectroscopy, and security since it includes the fingerprint absorption of numerous molecular gases. However, the implementation of VBGs into bulk fluoride glasses represents a challenging task due to the thermal properties of such glasses. Indeed, in comparison to fused silica, they have a significantly lower glass-transition temperature (265°C), a much larger thermal expansion coefficient (200×10^{-7}/K), and a lower thermal diffusivity (2.4×10^{-3} cm^2/s). This can lead to thermal instabilities when a tightly focused fs-laser beam interacts with the fluoride glass [12]. Specifically in ZBLAN glass (abbreviation for $ZrF_4 - BaF_2 - LaF_3 - AlF_3 - NaF$, the most common fluoride glass composition), optical devices have been so far only implemented into fibers in the form of fiber Bragg gratings (FBGs) [13] or long-period fiber gratings (LPGs) [14]. An approach to implement their counterpart, namely VBGs, into fluoride bulk glasses is still missing most likely due to the strict requirements on the period stability along with the challenges of volume modifications mentioned above. Such components working from the UV to the mid-IR wavelength region are required for high-end applications such as pulse compression in mid-IR chirped-pulse amplification (CPA) systems or wavelength filtering for hyperspectral imaging.

In this Letter, we report what we believe are the first fs-laser inscribed VBGs in bulk fluoride glasses. The gratings described in this contribution reveal good diffraction and reflection efficiencies in the mid-IR region, and their spectra show good agreement with numerical modeling. The gratings' homogeneity and higher-order reflectivities are also investigated. Finally, the influence of thermal annealing is analyzed.

For the VBG inscription process, we apply ultrashort laser pulses (100 fs) and the scanning phase-mask technique to obtain a high period stability [9]. The 800 nm beam of a CPA Ti:sapphire-laser (*Spitfire, Spectra-Physics*) with a diameter of 4.8 mm is focused by an acylindrical lens ($f = 12$ mm) through a phase mask into the fluoride glass sample as illustrated in
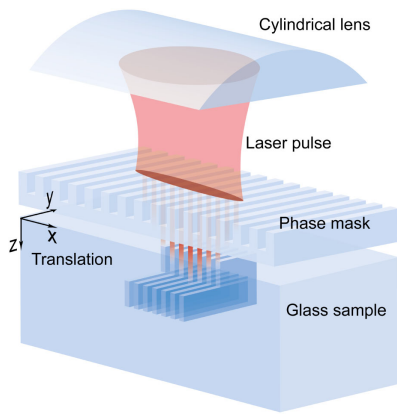
Fig. 1.   Illustration of the VBG inscription setup using a cylindrical lens and the multilayer scanning phase-mask technique.

Fig. 1. The phase mask with a uniform period of 1.9 μm was used to obtain a first-order reflection peak around a wavelength of 2.8 μm. The undoped fluoride glass samples (*Le Verre Fluoré Inc.*) were cut into pieces with dimensions of $3 \times 3 \times 10$ mm, and their faces were polished. While the lens is focusing in only one direction, the phase mask is diffracting in the other, generating an interference pattern with half of the mask periodicity. By translating the sample and the mask together underneath the beam, the size of the grating can be extended to an almost arbitrary size without causing significant stitching errors [9]. The VBG is inscribed over the desired volume thanks to a layer-writing approach. The fs-beam is first focused at the bottom position of the grating, and both the bulk and the phase mask are translated exclusively along the y axis in order to inscribe the first layer (see Fig. 1). Once the required width is covered, the glass sample and the mask are moved down in z to focus the beam slightly higher in the bulk, and the previous process is repeated to inscribe a new layer. After writing a predetermined number of layers, the glass sample and the phase mask can be moved in the x direction to inscribe another VBG right next to the first one and therefore obtain a longer VBG.

After thorough optimization tests, the final VBGs were inscribed with a laser repetition rate of 100 Hz, a pulse energy of 520 μJ, and with a double-pass exposure as it can induce larger refractive-index modification amplitudes Δn_{AC} [9]. Such a low repetition rate was chosen, since poorer gratings were obtained when the laser was operated at 1 kHz. Even though this last repetition rate is generally known to not be in the heat-accumulation regime in standard silicate glasses, we believe that our current beam scanning technique used to obtain such large Bragg structures does not allow us to scan the fs-beam fast enough to limit detrimental heat accumulation effects in the focal area of the fluoride glass samples [12]. A distance of 22 μm was kept between each layer in order to ensure a smooth index modulation over the grating's height. The writing beam was scanned at a speed of 0.6 mm/min along the y axis and over the 2 mm width of the layers. That process was repeated for 67 layers to inscribe gratings over a height of 1.5 mm. A distance of 170 μm was kept between the top surface and the last written layer in order to prevent the focused beam from damaging the bulk surface. Two final VBGs were written over lengths of 3 and 10 mm. This latter length was obtained by inscribing four gratings next to each other in the same bulk sample, each spaced
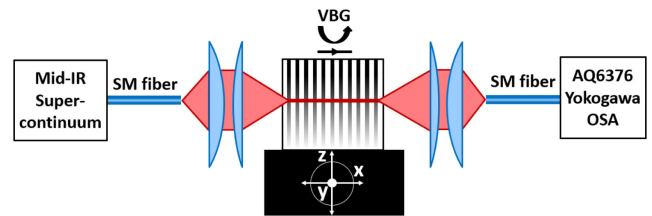

Fig. 2.   Setup for measuring the transmission spectrum of the VBGs. Mid-IR, mid-infrared; SM, single-mode; VBG, volume Bragg grating; OSA, optical spectrum analyzer.

by 2 mm in the x axis to ensure a sufficient overlap between themselves.

The setup shown in Fig. 2 was then used to probe the VBGs' different reflection orders. For that matter, we employed our in-house-built all-fiber supercontinuum source covering the wavelength range from 2 up to 4 μm to study the gratings' first diffraction order at normal incidence with regards to the fringe plane. Higher diffraction orders were probed with a commercial supercontinuum source (*SuperK, NKT Photonics*) covering from 0.5 up to 2.4 μm. The broadband light of these characterization sources is carried to the setup by means of a single-mode fiber. It is then focused inside the glass bulk thanks to a set of two CaF$_2$ lenses. Their focal lengths are chosen to obtain the smallest beam possible while keeping a confocal parameter (twice the Rayleigh range) at the wavelength of interest at least as long as the probed VBG. Such a small beam area is desired since we wanted to evaluate the Δn_{AC} homogeneity of the refractive-index modulation amplitude over the grating' cross section. The sample was therefore positioned with a 3D translation stage and a rotating stage to ensure an efficient alignment and an optimized coupling. The transmitted light is then refocused into a single-mode fiber connected to an optical spectrum analyzer (OSA). For the measurement of the VBGs' first diffraction order, a mid-IR OSA (*AQ6376, Yokogawa*) that spans from 1.5 to 3.4 μm was used.

The transmission spectra around the first-order resonance of the two VBGs are displayed in Figs. 3 and 4. Clear transmission dips are observed around 2.836 μm as expected from the choice of the phase-mask period by considering a refractive index of ∼1.49 for fluoride glass near 2.8 μm. A 0.7 nm offset is observed between the peak wavelengths of both VBGs, probably due to a small angle difference between the probing beam and the gratings' fringes. The transmission spectra were normalized according to a spectrum obtained by sending the beam through the bulk but outside the grating region. As seen in Fig. 3, the 3-mm-long VBG exhibits a transmission dip of −5 dB at the resonant wavelength, which was probed by sending a ∼75 μm-diameter beam over the region of the VBG closer to the top surface of its bulk. By fitting this spectrum with an in-house-developed simulation tool for VBGs, we were able to infer a peak Δn_{AC} of 5.1×10^{-4}. Those simulations are based on the model of rigorous coupled wave analysis [15]. In order to mimic the experimental conditions as closely as possible, the Δn_{AC} envelope of the gratings is given by the intensity profile of the fs-beam revealing a Gaussian-apodized profile with additional modulations. This is accompanied by a small Gaussian deformation of the average refractive index (Δn_{DC}). In addition, a slight divergency of the probing beam is assumed to properly fit the asymmetric shape of the spectrum. A slightly longer grating
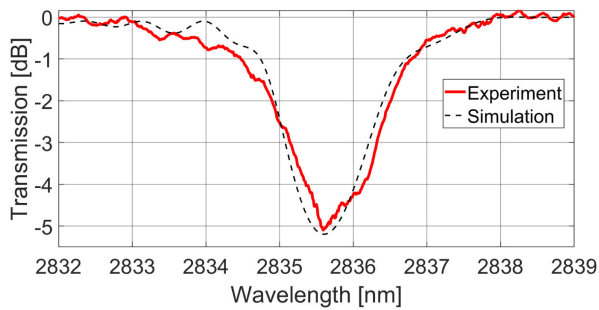
Fig. 3. Measured and simulated first-order transmission spectra of the 3-mm-long VBG. For the simulations, $\Delta n_{AC} = 5.1 \times 10^{-4}$, and Gaussian shapes for Δn_{AC} and Δn_{DC} are assumed.
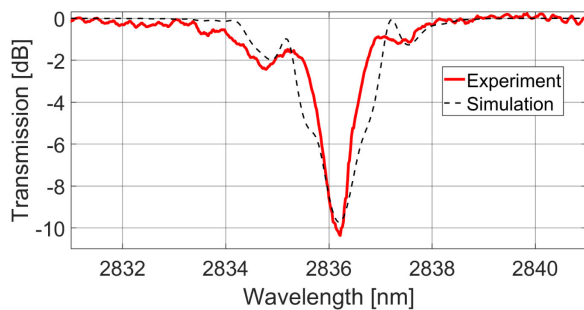

Fig. 4. Measured and simulated first-order transmission spectra of the 10-mm-long VBG. For the simulations, $\Delta n_{AC} = 3.2 \times 10^{-4}$, and Gaussian shapes for Δn_{AC} and Δn_{DC} are assumed.

length of 3.8 mm was also assumed. Since no commercial mid-IR fiber couplers are available, the first-order peak reflectivity of the VBG cannot be directly probed. However, its value can be inferred from the dip of its transmission spectrum given the good agreement between the simulations and the experimental results and by assuming negligible photoinduced losses. Such assumption is justified as no significant out-of-band losses were observed on the normalized spectrum of Fig. 3 and since negligible losses have also been previously reported for mid-IR FBGs inscribed in fluoride glass fibers with the phase-mask technique [16]. We can therefore assume from the −5 dB transmission dip that this VBG has a first-order peak reflectivity of about 70%. In the case of the 10-mm-long VBG's spectrum shown in Fig. 4 exhibiting a −10 dB transmission dip, we can infer a peak reflectivity of 90%. It was probed with a ∼150 μm-diameter beam, which was also sent on the VBG's top layers. The FWHM of the resonance is 1.1 nm and was measured with the highest OSA resolution of 0.1 nm. From the fitting of that spectrum obtained with the simulation code and by assuming a grating length of 8 mm, we calculated a peak Δn_{AC} of 3.2×10^{-4}. This value is almost 40% lower than that calculated for the shorter VBG, even if both VBGs were inscribed with the same inscription parameters. Such a discrepancy could hint at a potential poor Δn_{AC} homogeneity over the VBGs' cross section given that this longer grating was probed with a much larger beam than for the other one.

The Δn_{AC} homogeneity was studied by measuring the first-order transmission dip of the 10-mm-long VBG at different positions over its cross section. The 3D translation stage shown in Fig. 2 was used to move the sample along the z axis in order
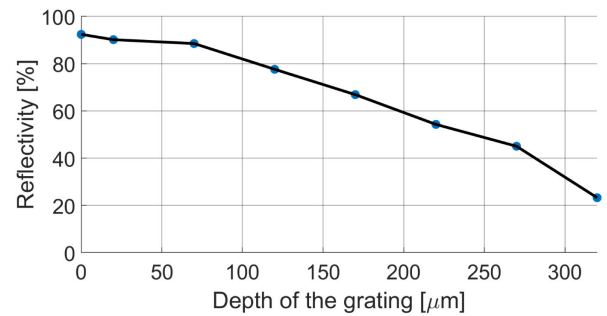

Fig. 5. First-order peak reflectivity of the 10-mm-long VBG measured at different height positions.

to measure the transmitted spectrum of the 150-μm-diameter probing beam at different height positions inside the bulk. The results summarized in Fig. 5 confirm that there is indeed a strong grating-strength gradient in that axis. The peak reflectivity evaluated from the transmission dip drops from 90% at the top of the grating to 23% at a depth of 320 μm. It is especially surprising given that a 1.5 mm scanning range was used for the grating's height during the inscription process. Such inhomogeneity can be explained by the spherical aberration at the interface between air and the glass bulk. It distorts the focus and consequently reduces the intensity at the focal point. This effect becomes more important with increasing focal depth inside the sample [17]. Thus, Δn_{AC} is expected to decrease from the top to the bottom layer. Taking the probe beam diameter of 150 μm into account, this means that Δn_{AC} does not only depend on position but is also averaged over the probing beam area. Therefore, the maximum value of photoinduced Δn_{AC} extrapolated from the transmission measurements is underestimated. In the future, the VBGs' homogeneity could be greatly improved by increasing the pulse energy for the bottom layers or by precompensating the aberrations on the writing beam with a spatial light modulator for instance [18]. Similar measurements were also conducted to study the grating's homogeneity over the y axis. A significantly more uniform reflection efficiency with a relative RMS deviation of 6% was observed along the whole 2 mm width of the VBG. It is worth noting that by improving the gratings' depth homogeneity and by further optimizing the writing parameters, Δn_{AC} of the order of 1×10^{-3}, as reported in [13], could be obtained over the whole cross section of the VBG. Those improvements along with larger grating lengths will allow us to increase even more the peak reflectivity of the resulting VBGs.

The 3-mm-long VBG was then probed at the second reflection order. In this case, we used a 2×1 single-mode fiber coupler to send the supercontinuum source' beam to the characterization setup of Fig. 2. The third branch of the coupler was connected to an OSA (*AQ6370C, Yokogawa*) to obtain the reflection spectrum shown in Fig. 6. It was normalized according to the peak reflectivity inferred from the dip of its transmission spectrum also displayed in Fig. 6. The baseline of the reflection spectrum comes from the parasite reflections of the free-space characterization setup. Still, a good agreement is observed between the reflection and the transmission spectra with regards to their FWHM and the wavelength positions of their sidelobes. This tends to confirm the validity of calculating the VBGs' peak reflectivity directly from their transmission dip as reported before. Those results also confirm that the
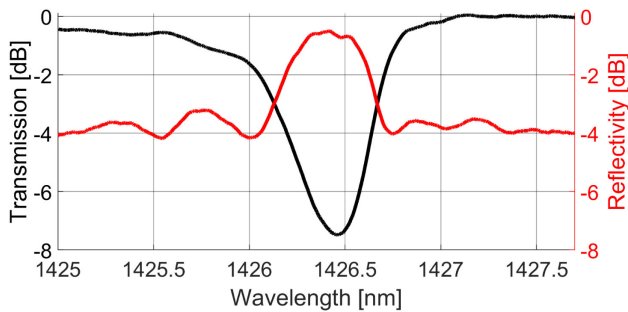
Fig. 6. Second-order transmission and reflectivity spectra of the 3-mm-long VBG.

phase-mask approach allows for the inscription of VBGs with a very stable period along their length and that they can thus be used as highly effective reflectors. An 83% reflectivity at a peak wavelength of 1426 nm was obtained with a ∼70 µm-diameter beam. The smaller baseline seen on the short-wavelength side of the transmission spectrum is likely to come from a bad spectrum normalization due to the free-space nature of the setup. This was in fact not observed with the other diffraction orders' spectra. With the same VBG, a 70% third-order reflection peak was also measured at 953 nm with a ∼50 µm beam diameter suggesting that even higher orders could be observed. These strong higher-order diffraction peaks result from the nonsinusoidal refractive index profile of the photoinduced gratings [19].

While the spectra shown in Figs. 3 and 4 were measured six months after the inscription of the gratings, confirming that they can maintain a strong diffraction efficiency on the long-term basis, in addition we also analyzed the effect of thermal annealing. Thermal stability of the fluoride glass VBGs is indeed an important matter for any potential application. Thus, we measured the peak Δn_{AC} of a grating inscribed with the optimized parameters described above, after annealing it at different temperatures for 30 min. As seen in Fig. 7, the induced Δn_{AC} decreases by 70% from its initial value after a thermal treatment at 200°C. Similar observations explained by the low glass-transition temperature of fluoride glasses have already been reported for FBGs [13] and LPGs [14] inscribed in such material. Those measurements were conducted right after the inscription of the VBG. The peak Δn_{AC} values were calculated by using the grating as a transmitting VBG and measuring its diffraction efficiency of a He–Ne beam according to Refs. [9,20] given that the mid-IR characterization setup was not available at that time. Further thermal annealing tests are under investigation to study the VBGs' long-term stability.
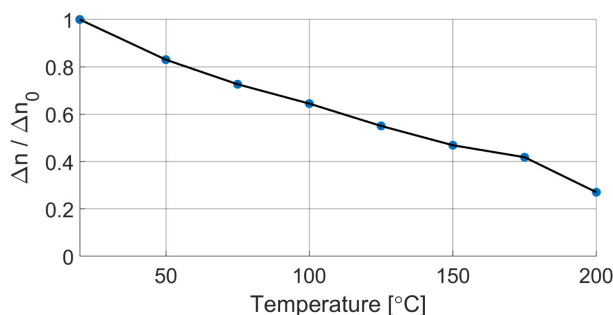

Fig. 7. Evolution of the VBG's normalized Δn_{AC} for different annealing temperatures each held constant for 30 min.

In summary, we have reported the first VBGs ever written inside multicomponent fluoride glass. They were inscribed in undoped bulks of that material with an IR-fs-beam and the multilayer scanning phase-mask technique. That approach circumvents stitching errors and allows for the writing of highly effective VBGs. We were indeed able to infer from their transmission spectra that the VBGs exhibited strong first-order reflection peaks in the mid-IR. Despite a strong inhomogeneity along the height of the inscribed VBGs, high reflectivity values of 70% and 90% were obtained at a wavelength of 2.8 µm for VBGs with lengths of 3 mm and 10 mm, respectively. Strong higher-order reflections were also observed. This work enables the use of VBGs in the mid-IR spectral region.

Disclosures. The authors declare no conflicts of interest.

REFERENCES

1. A. Sevian, O. Andrusyak, I. Ciapurin, V. Smirnov, G. Venus, and L. Glebov, Opt. Lett. **33**, 384 (2008).
2. D. Richter, M. P. Siems, W. J. Middents, M. Heck, T. A. Goebel, C. Matzdorf, R. G. Krämer, A. Tünnermann, and S. Nolte, Opt. Lett. **42**, 623 (2017).
3. O. M. Efimov, L. B. Glebov, L. N. Glebova, K. C. Richardson, and V. I. Smirnov, Appl. Opt. **38**, 619 (1999).
4. K. Yamada, W. Watanabe, K. Kintaka, J. Nishii, and K. Itoh, Jpn. J. Appl. Phys. **42**, 6916 (2003).
5. D. Grobnic, S. J. Mihailov, C. W. Smelser, M. Becker, and M. W. Rothhardt, IEEE Photon. Technol. Lett. **18**, 1403 (2006).
6. Y. Matushiro, S. Juodkazis, K. Hatanaka, and W. Watanabe, Opt. Lett. **42**, 1632 (2017).
7. D. G. MacLachlan, R. R. Thomson, C. R. Cunningham, and D. Lee, Opt. Mater. Express **3**, 1616 (2013).
8. K. Itoh, W. Watanabe, S. Nolte, and C. B. Schaffer, MRS Bull. **31**, 620 (2006).
9. C. Voigtländer, D. Richter, J. Thomas, A. Tünnermann, and S. Nolte, Appl. Phys. A **102**, 35 (2011).
10. C. W. Smelser, D. Grobnic, and S. J. Mihailov, Opt. Lett. **29**, 1730 (2004).
11. S. D. Jackson, Nat. Photonics **6**, 423 (2012).
12. J.-P. Bérubé, M. Bernier, and R. Vallée, Opt. Mater. Express **3**, 598 (2013).
13. M. Bernier, D. Faucher, R. Vallée, A. Saliminia, G. Androz, Y. Sheng, and S. Chin, Opt. Lett. **32**, 454 (2007).
14. M. Heck, S. Nolte, A. Tünnermann, R. Vallée, and M. Bernier, Opt. Lett. **43**, 1994 (2018).
15. M. Moharam and T. Gaylord, J. Opt. Soc. Am. **71**, 811 (1981).
16. D. Faucher, M. Bernier, G. Androz, N. Caron, and R. Vallée, Opt. Lett. **36**, 1104 (2011).
17. A. Marcinkevičius, V. Mizeikis, S. Juodkazis, S. Matsuo, and H. Misawa, Appl. Phys. A **76**, 257 (2003).
18. P. Salter, M. Baum, I. Alexeev, M. Schmidt, and M. Booth, Opt. Express **22**, 17644 (2014).
19. C. W. Smelser, S. J. Mihailov, and D. Grobnic, Opt. Lett. **32**, 1453 (2007).
20. I. V. Ciapurin, L. B. Glebov, and V. I. Smirnov, Opt. Eng. **45**, 015802 (2006).